

Exploring Rotation and Scale Invariant Features in Image Plagiarism Detection Using Manifold-Ranking Algorithm

Simindokht Jahangard*

MSc, Department of Computer Engineering, Amirkabir University of Technology (Tehran Polytechnic)

*Corresponding author E-mail: s.jahangard66@gmail.com

Abstract

Plagiarism, as a crucial offense especially in academia, not only is well-known problem in text but also is becoming widespread in image. In this work, the performance of manifold-ranking, known as robust method among semi-supervised methods, has been investigated by using twelve different features. As its high performance is attributed to the quality of constructed graph, we applied robust k-regular nearest neighbor (k-RNN) graph in the framework of manifold-ranking based retrieval. Among all tested feature point detectors and descriptors, Root-SIFT, the feature point ones, due to it is invariant to an array of image transforms, is the most reliable feature for calculating image similarity. The database consisting of images from scientific papers containing four popular benchmark test images served to these methods.

Keywords: image plagiarism, image retrieval, feature extracting, k-regular nearest neighbor graph, manifold-ranking.

1. Introduction

With the spread of digital data, plagiarism is very important subject that has received much attention over the past decade. Plagiarism detection is the process of locating instances of plagiarism within a corpus of documents. Extensive use of computer and advent of internet and software has made it easier to plagiarize the work of others. While plagiarism can occur in any field, most cases of plagiarism are found in academic documents. Recent research works has been conducted merely based on textual information of documents, ignoring other media during the similarity analysis. Extrinsic text plagiarism detection based on current state of art techniques, MultiLayer Self-Organizing Map (MLSOM) with tree-structured data, the Levenshtein distance and Smith-Waterman algorithm, a Nearest Neighbor (NN) search for measuring semantic similarity and text syntactical structures were used for text plagiarism detection in [1-4] and [5] respectively which are good examples in this area. Pictures play an important role in recent documents. They are inseparable part of document plagiarism. The common image plagiarism technique is mainly divided into image retouching, copy-paste and copy-move groups. Copy-move forgery is performed by copying small patch from another part of image to disappear an object in image. Retouching is the process of improving or repairing the image without changing noticeable modification of the content of image. Copy-move forgery account for majority of image plagiarism detection. Consequently, it is more discussed in present essay. In order to compute the similarity between images, a high-performance image retrieval system is needed. The large volume of data and image datasets is one of the significant challenges in image retrieval. To deal with this problem, graph-based retrieval systems are developed to alleviate the need for large amount of memory. Bin Wang et al [6] proposed a new graph

structure for retrieval-based manifold-ranking. They showed that manifold-ranking algorithm applied on k-Regular Nearest Neighbor (k-RNN) graph structure outperforms the state-of-the-art algorithms that use traditional graph structures. The main function of manifold-ranking is to re-calculate the ranking score of the images retrieved as a result of a query. In addition to applying manifold-ranking algorithm on k-RNN graph, there exist several other variations of manifold-ranking algorithm that are proposed for text-based applications [7-10]. Nevertheless, the manifold-ranking algorithm suffers from some drawbacks which limits its applicability to Content Based Image Retrieval (CBIR) on very large datasets. Except a few research works [11, 12], conducted on image plagiarism in documents, there is an insufficient number of studies comparing the effect of different image features on the effectiveness of this algorithm. This paper aims at evaluating the performance of manifold-ranking based in image retrieval systems by using k-RNN graph to find identical images scaled and rotated. It investigates the effect of robust scale and rotation invariant features that are used to calculate the similarity between the images in the k-RNN graph. In other words, extraction of appropriate image features and selection of a robust measure to identify the similar images is required for comparing similarity of two document included pictures. In the current study, a number of image descriptors including Scale Invariant Feature Transform (SIFT) [13], RootSIFT [14], Speed Up Robust Features (SURF) [15], Geometric Blur [16], Scene Gist [17], Color Moments [18], Color Correlogram [19], Gabor filter [20, 21], Biologically inspired hierarchical model [22], Edge Histogram Descriptor (EHD) [23, 24], Hue Saturation Value (HSV) and Local Binary Pattern Histogram Fourier Features (LBP-HF) [25] have been examined. The feature detectors and descriptors are selected based on their application in finding similar images in a corpus of scientific documents using manifold-ranking and k-

RNN graph. The process of feature extraction and image retrieval is shown in Fig.1.

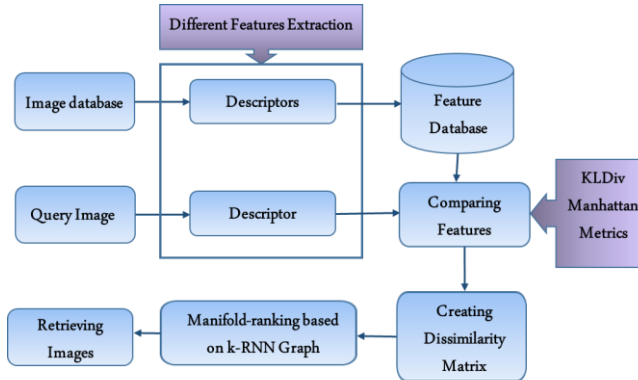


Fig. 1: Flow of image retrieval system using k-RNN graph

We organize the rest of this article as follows: we present a brief review on related works in the second section. In the third section, the method evaluating the performance of image retrieval against the extracted features is explained. The experimental results and their discussion are presented in section four and section five provides conclusions.

2. Related Works

The importance of plagiarism detection in recent years, has motivated several researchers to develop various plagiarism detection techniques. Some of them use the degree of resemblance between images contained in the documents as a criterion for measuring the similarity of the documents. In order to detect copy-move forgery the blur moment invariants techniques was used by Mahdian and Saic [26]. The robustness of their work is shown when they add noise, change contrast and degrade in the duplicated regions. However, their method suffers from high computation time. Mohammadian et al. [27] added Zernik Moment which is invariant to rotation in contrast to SIFT method which fails to find flat copied regions, i.e. regions with flat texture. They found that the combination of SIFT and Zernik moment can be appropriately used to detect all types of copied regions in an image. Their method is limited in determining potential geometric transformations. Popescu and Farid [28] applied Principal Component Analysis (PCA) to discover copy-move plagiarism. After dividing image into blocks, they used PCA to represent each block and created a vector for each block in order to detect forgeries. They organized it lexicographically and match vectors. However, their method is just for gray scaled pictures and the potency decreases because of small size of blocks. In addition, the its performance decline when the quality of image is low. The new method based on Singular Value Decomposition (SVD) was suggested by Ting and Rang-ding [29] to find and locate duplication regions. They substitute a method of k-tree fast enough for exhaustive searching to match feature. Weak performance in JPEG compression, along with failing to detect copied and pasted part is its problem. A novel methodology of copy-move plagiarism detection is proposed by Zimba and Xingming [30]. Initially, Discrete Wavelet Transform (DWT) is applied to entire gray image divided into various overlapping blocks. Eigen price decomposition is performed on the blocks. Their algorithm is impractical when duplicated region is larger than the block size. Bravo-Solorio and Nandi [31] provided a technique to detect scaled, rotated and reflected forgeries. The need of refinement to scale heap of matches back is their drawback. Recently, A copy-move plagiarism detection method in an extremely parallel setting is proposed by Sridevi et al [32]. Their method proved to have suboptimal performance in dealing with color images.

In the following section, several well-known image features commonly used in the existing research works, have been reviewed. Huang et al. [33] provided a method using SIFT to detect

copy-move forgery in images. In order to measure similarity, descriptors match pasted region and copied region in search of any possible forgery in digital images. Amerini et al. [34] presented a novel approach for detecting copy-move forgeries using SIFT features which localizes the accurate forgery utilizing J-Linkage algorithm. This algorithm has a significant clustering in the domain of geometric transformation for grouping SIFT key points spatially close. Some researchers such as Arandjelovic et al. [14] introduced a new method by using Rootsift for object retrieval in large scale image dataset. Pandey et al. [35] designed a method that uses SURF and SIFT robust in detecting copy-moved regions. Prasad et al. [36] compared the SURF and hybrid features such as SURF-HOG and SIFT-HOG, Histogram of Oriented Gradients (HOG), and the copy-move forgery detection using image features like SIFT, Lee [37] provided a new image searching method extracting features and combine Advanced Speed up Robust Feature (ASURF) and Domain Color Descriptor (DCD). In comparison with open source OpenSURF, their algorithm exhibits a dramatic improvement in retrieval effectiveness. Jau-Ling [38] used primitives of color moments to introduce a color image retrieval technique. They divided an image into blocks, extracted the color moment of each block and then clustered them into some classes. Malviya et al. [39] exploited a CBIR feature extraction scheme to detect a typical forgery by employing Auto Correlogram their work has significant accuracy to detect the forged region. They focus on color content in forges image and extract features and then analyze the color moments and HSV color space of the tampered image [40]. Su et al. [41] made a comparison between RGB and HSV color space for image retrieval. Yohannan et al. [42] provided a method to detect copy-move forged pictures. They employed a set of feature vectors obtained from the responses of the Gabor filters for each overlapping patch of the image. Lee [43] presented an efficient method to tackle copy-move forgery problem. They divide the forged image into overlapping fixed-size blocks, and then apply Gabor filter to each block. In the next step, they used Histogram of Oriented Gabor Magnitude (HOGM) of overlapping blocks and extracted the statistical features for similarity measurement. Agarwal et al. [44] proposed a novel method for CBIR based on DWT and EHD. After applying wavelet transform, the information of dominant edge orientations is gathered by using EHD on wavelet coefficients they showed that, by combining the DWT and EHD techniques the performance of the CBIR system has been increased. Li et al. [45] also presented a method filtering and dividing the image into overlapping circular blocks, firstly. Then, they use rotation invariant uniform LBP to extract the features of the circular blocks. Finally, the forged regions can be located by comparing the feature vectors calculated in the previous step. Ustubioglu et al. [46] proposed a LBP-DCT based copy-move algorithm to detect forgery. The image is divided into overlapping blocks followed by using LBP to label each block. In the next step, DCT (Discrete Cosine Transform) is used to transfer blocks into frequency domain. After signing values of the zigzag scanned block, the features are lexicographically sorted to determine the forged blocks. It can be concluded from the literature that some features are robust to some basic affine transforms, e.g. rotation and scaling. These features are more suitable to be used in copy-move forgery detection specifically for scientific papers. The next section aims at proposing a method to identify the effect of incorporating each feature in constructing the k-RNN graph and detecting plagiarized articles based on the similarity of their images using manifold-ranking algorithm.

3. The Proposed Method

We simplify our problem to the task of finding a set of robust features and identifying suitable features which provide more discrimination between the forged and authentic images. To achieve our goal, the Kullback-Leibler Divergence (KLDiv) and Manhattan distance were chosen as criteria to compute the dis-

similarity between each pair of images in the dataset. In the next step, the dissimilarity matrix is created based on the selected distance measure providing the weights of edges in k-RNN graph. Then the manifold-ranking algorithm is used to update the weights of the edges connecting the query image to its neighbors. The final result of a query consists of a set of most similar images and the score of each retrieved image. The details of the main steps of our work are described below.

3.1. Overview of Image Feature Extraction

The image feature detection and extraction have been known as the main steps of a massive variety of image processing applications. The efficiency of content-based image retrieval systems is highly dependent on the image descriptors used for calculating the similarity of the images. Our work is motivated by applications in plagiarism detection where similarity of images included in document serves to compare two documents. It requires appropriate extraction of image features and selection of robust method to compare these features. The image feature descriptors are divided in two main groups: a) local and b) global descriptors. In the following, we briefly present some typical local and global image descriptors:

3.1.1. Local descriptors

Local descriptors focus on parts of image that discriminative information is more prominent and compute around the interest points.

- **SIFT**

SIFT, a stable and robust image feature, is invariant to illumination, scale and rotation, proposed by Lowe [13]. In our work, for every image SIFT key points and feature vectors are generated. Each key point has an associated feature vector composed of 128 scalar values. These vectors are combined into a single matrix containing all the feature vectors for each image. Kmeans method was used to cluster vectors and the number of clusters is selected to be 15. Then, a histogram for each image is created.

- **RootSIFT**

A new version of SIFT called RootSIFT, was proposed by Arandjelovic et al. [14]. RootSIFT is a square root of the L1 normalized SIFT vector. The formula is defined

$$RootSIFT = \sqrt{\frac{SIFT}{\sum SIFT}} \quad (1)$$

Where SIFT is the L1 normalized SIFT vector. Akin to SIFT, its histogram is calculated that is discussed in previous. The only difference is the way of extracting feature vector which is normalized using (1).

- **SURF**

SURF is a speed up version of SIFT introduced by Bay et al. [15]. Having lower dimension, SURF have higher speed of calculating and matching. SURF can be used in the same way as SIFT except in length of scalar values. It detects landmark points in an image and describe the points by a vector robust against a rotation, scaling and noise.

3.1.2. Global descriptors

Global descriptor is a single descriptor capturing entire information of the visual content. The global descriptors can also be divided into three main types: color, texture and shape category.

3.1.2.1. Color

Our human visual perception system relies on color spatial distribution of color in an image can be used to create a color descriptor.

- **HSV**

HSV is the most common representations of points in an RGB color model. HSV histogram shows the distribution of colors in an image used in many aspects of image retrieval. In our algorithm, we quantize image into 8x2x2 equal bins in HSV color space and a 1x32 vector is the output showing features extracted from HSV.

- **Color Moments**

To represent color distribution Color Moments are another method. includes three main moments: 1) Mean: the average value of all pixels. 2) Standard deviation: representing the disparity of color values of the distribution. 3) Skewness: capture the asymmetry degree in the distribution [18, 38].

- **Color Correlogram**

Color Correlogram defined by Huang et al shows how pixels with a given color are spatially disturbed in an image [19]. This feature distills the spatial correlation of colors used for indexing and comparison. In our work we used the vector in which the color distribution in different distances is calculated. The output was a straight vector exhibiting the probabilities of occurrence of 64 quantized colors. Its total dimension is 64nx1; where n is the number of different inf-norm distances.

3.1.2. Texture

Texture can be defined as the visual pattern. There are many texture feature extraction techniques that here we refer to some of them.

- **LBP**

LBP descriptors are used for retrieval and texture classification proposed by Ojala et al. [48]. LBP considers the neighbors of a pixel and generate a bit-code from the binary derivatives of a pixel. After generating the LBP-code is generated for all pixel and then, the texture image is represented by the histogram of LBP codes. In this article, LBP-HF is computed from discrete Fourier transform of LBP histogram invariant to rotation [25].

- **EHD**

The concept of EHD rely on edge distribution. It is described as a form of histogram based on local edge distribution in an image which is utilized for image matching [23, 24]. In our work, five various masks (horizontal, vertical, diagonal, anti-diagonal and non-directional) have been used to create the edge images. We divided images into blocks and compute their histograms.

- **Gabor filter**

Gabor filter that its function is edge detection works like human visual system by applying linear filter on image. Gabor filter gives set of strong response for locations of the target images that have structures in this given direction. In addition, these filters optimize localization properties in both spatial and frequency domain [20, 21]. In this article, this method calculates Gabor features and mean-squared energy and mean amplitude. We used five number of wavelet scales and six number of filter orientations. The convolutions are done via the Fast Fourier Transform (FFT).

- **Biologically inspired hierarchical model (Jarrett)**

Biologically inspired hierarchical model tested by Jarrett et al. [22] is what they describe as Fcsg-Rabs-N-Pa using one stage of random filters with no learning. The number of filters, filter size and down sample can be various. These filters generated from white noise, convolved with each image. Therefore, for each image there are 64 new images, and histograms are created from the raw pixel values of each new image.

- **Geometric Blur**

Geometric blur, implemented by Berg [16], is used to compare two signals when geometric distortion exists. It matches shapes based on geometric blur descriptors to recognize objects. Geometric blur differs in two ways from the original description. The filter size is slightly smaller: 9px. This was done because the images that were originally tested with this program were of lower resolution than used by Berg. The sub-sampling diagram still follows what was proposed in the paper as closely as possible. The program also differs in that it deals with the point correspondence problem, determining which points between images are considered matching by simply using the nearest neighbor point, instead of what was proposed by Berg. Neither of these differences seem to prevent the results from being highly clustered, typically separating images into clear distinctive groups.

3.1.2.3. Gist

The GIST descriptor proposed in [17] comes from developing a low-dimensional global image representation of the scene which does not require any form of segmentation.

- **Scene Gist**

This method proposed by Oliva [49]. To recognize real-world scenes, Scene Gist is a model bypassing the segmentation and the processing of individual objects or regions. Our algorithm convolves the image with several Gabor filters at 4 orientations producing maps of the same size as the input image. Then it divides each map into 4 blocks and averages the feature values within each block. Finally, it concatenates the averaged values of all feature maps, resulting in Gist descriptors.

3.2. Compare Features and Constitution of Dissimilarity Matrix

$$D_{L1}(A, B) = \sum_{i=1}^n |a_i - b_i| \quad (2)$$

$$D_{KL}(A, B) = \sum_{i=1}^n a_i \log \frac{a_i}{b_i} \quad (3)$$

In this experience, we used KLDiv measurement metric for SIFT, RootSIFT, SURF, Scene Gist, Geometric Blur and Jarrett. Manhattan metric is also used for ColorMoment, Gabor, EHD, HSV, Color Correlogram and LBP-HF. After measuring distance for each pair of images, each distance is saved in a matrix named dissimilarity matrix in which each element shows the dissimilarity of a pair of images. Digits in the dissimilarity matrix are positive and the biggest number shows the lowest similarity and 0 shows the highest similarity. It is obvious that the elements in the main diagonal must be 0 or near 0. After computing the dissimilarity matrix, the k-RNN graph has to be created. In order to better analyze, the performance of the methods has been predicted in Table 1, the average of KLDiv distances has been calculated for two separate datasets for the first six methods. The first dataset (Relevant Pic) contains 20 images of query images rotated and scaled and the second dataset (Irrelevant Pic) contains 20 images that are quite different from the query image. In order to enhance the accuracy of the investigation, four benchmark images shown in Fig. 2, employed and the averages of all four images were calculated. Using the KLDiv measurement, we see that the SURF method has the greatest difference. Therefore, it is speculated that its performance would probably be considerable. Table 2, akin to Table 1, shows the second six methods compared by Manhattan distance. Among the second six methods, we can see that the HSV method has the highest difference. Hence, it would maybe perform well.

Table 1. Pre-evaluation of methods measured by KLDIV metric

	KLDIV					
	SIFT	RootSIFT	Jarrett	SURF	Geometric Blur	Scene Gist
Relevant Pic Mean	0.0816	0.0915	0.3215	0.418275	0.0039	0.67855
Irrelevant Pic Mean	1.7523	1.8805	4.6209	7.232525	0.0039	1.06075
Difference Value	1.6707	1.789	4.2994	6.81425	0	0.3822

Table 2. Pre-evaluation of methods measured by Manhattan metric

	Manhattan Distance					
	EHD	LBP-F	HSV	ColorMoment	Gabor	ColorCorre
Relevant Pic Mean	0.5923	0.58915	0.106	0.053925	0.352025	0.412725
Irrelevant Pic Mean	0.757725	0.749475	1.46515	0.20545	0.61155	0.58145
Difference Value	0.165425	0.160325	1.35915	0.200575	0.259525	0.168725

Described in the previous section, after extracting features from each picture and obtaining its descriptors, the next step for creating a dissimilarity matrix is deserving a reliable measurement. Manhattan measurement metric and KLDiv, a measure of the non-symmetric difference between two probability distributions [50], are utilized for calculating the distance. Below shows Manhattan (1) and KLDiv (2) criteria in which $A = \{a_1, \dots, a_n\}$ and $B = \{b_1, \dots, b_n\}$ are feature vectors with n bins.



Fig. 2: Four test (reference) images: A - 'baboon', B - 'Lena', C - 'peppers', D - 'airplane'.

3.3. Creating k-RNN graph

In this section, we introduce the k-RNN graph and manifold method in more detail. To evaluate the performance of features, a k-RNN graph structure proposed by Bin Wang et al [1] is created. K-RNN graph structure in framework of manifold-ranking extends the functionality of manifold-ranking in retrieval systems.

3.3.1. The Concept of k-Regular Nearest Neighbor Graph

Compare with k-RNN graph, previous graphs like connected graph and KNN graph suffer from some limitations lead to low performance in manifold ranking. Therefore, in order to reserve merits of previous graphs and avoid their disadvantages, k-RNN is proposed. In k-RNN, an undirected graph, each vertex shows a data point in feature space X , and the distance $d(x_i, x_j)$ also represents their corresponding distance. KLDiv, Manhattan distance(L1), Euclidean distance(L2), Mahanobis and Chebychey(L ∞) distance can be considered as $d(x_i, x_j)$. The steps of construction method of k-RNN are proposed in Algorithm1 [6].

Algorithm 1. Constructing algorithm of k-RNN.

Input: m : the maximum degree of all the vertices;
 k : the average degree of all the vertex.
Output: the constructed k-RNN graph G .

- 1 Sort the pairwise distances of each points in ascending order, and record them in table T ;
- 2 Initialize the k-RNN graph G with no edge added;
- 3 Define integer value $averageDegree=0$;
- 4 Define integer value $maxDegree=k$;
- 5 **while** $averageDegree < k$ and $maxDegree < m$ **do**
- 6 **foreach** $edge$ in T **do**
- 7 Denote its two vertex as S and E ;
- 8 **if** S and E are $maxDegree$ nearest neighbors **then**
- 9 Add $edge$ to G ;
- 10 Remove $edge$ from T ;
- 11 **end**
- 12 **end**
- 13 $maxDegree = maxDegree + 1$;
- 14 Update $averageDegree$ as the average degree of G ;
- 15 **end**

3.4. Manifold-Ranking

One of the well-known graph-based ranking algorithm is manifold-ranking applied to retrieved image from multimedia databases effectively. Given a query image, the function of manifold-ranking is assigning score of all images in database. It exploits the relationships among the data in the form of graph is exploited, image here [8]. Recently, much research has been done on the manifold-ranking. Yang Wang et al. [9] proposed a method named Multi-Manifold Ranking (MMR) showing reliable performance on exploring the geometric structure of image set. Cheng Ta Hsieh et al. [51] introduced a 3D object retrieval method utilizing manifold-ranking and multiple features. Zhang et al. [52] provide a method to increase the speed of traditional manifold-ranking based method. One of the key factor is the quality of the constructed graph that have a significant impact on the performance of manifold-ranking [53]. Bing Wang et al. investigated various aspect of graph structures that affect the algorithm performance. They looked at the impact of connected graph and KNN graph in manifold-ranking and proposed a novel graph named k-RNN graph. Although there were many researches in area of manifold-ranking and k-RNN graph, the investigation in evaluating effect of various descriptors on k-RNN graph and manifold-ranking is limited. In this paper, we evaluate the effect of image feature descriptor on k-RNN graph. Algorithm 2 is the k-RNN-based manifold-ranking method.

Algorithm 2. Manifold-ranking algorithm based on k-RNN.

- 1 Calculate the pairwise L1 distance $d(x_i, x_j)$ of all the points;
- 2 Construct the k-RNN graph using Algorithm 1;
- 3 Form the affinity matrix W defined by
 $w_{ij} = \exp[-d^2(x_i, x_j)/2\sigma^2]$, if there is an edge linking x_i and x_j ;
- 4 Symmetrically normalize W by $S = D^{-1/2}WD^{-1/2}$, in which D is the diagonal matrix with (i,j) -element equal to the sum of the i -th row of W ;
- 5 Iterate $f(t+1) = \alpha Sf(t) + (1-\alpha)y$ until convergence, where α is a parameter in $[0,1]$;
- 6 Let f_i^* denote the limit of the sequence $f_i(t)$. Rank each point x_i according to its ranking score f_i^* (largest points are ranked first).

As discussed in Section 3.3, k-RNN graph will be created and final score is given to each image by manifold-ranking algorithm. The highest ranked images will be the retrieved images. The result will be discussed in next section.

4. Experiment Result

This section is dedicated to explain used dataset, some setup parameters in manifold-ranking, evaluation metrics and finally obtained results. To implement our method Matlab R2016b a computer of 2.6 GHz with memory of 16 GB was used.

4.1. Dataset

In order to validate, the image dataset in this article were extracted from 564 scientific articles, including the 1442 images stored in JPG format and their resolutions vary from (the smallest) 48x39 to (the biggest) 7500x4183 pixels. Some images can be seen in Fig.3. Four different benchmark images (Baboon, Lena, Pepper, Airplane) have been chosen (Fig.2 in section 3.4) and 20 forged images are created for each benchmark image which contain various resized, rotated and combined -both resized and rotated- images. We consider 5 scaled, 4 rotated and 11 combinations of scaled and rotated images. Some forged pictures can be seen in Fig.4. We made our test by considering the forged images found in real documents. Therefore, the created forged pictures are mostly scaled pictures rather than rotated images happening extremely rare in the case of document picture plagiarism. For more detail about dataset setup, please refer to Appendix A.

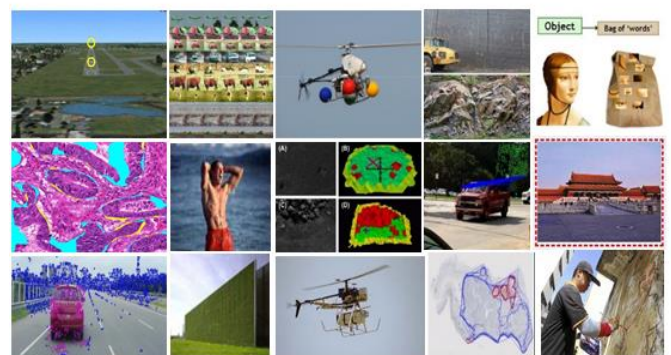


Fig. 3: Some images in dataset gotten from scientific articles



Fig. 4: Some forged pictures

4.2. Parameter Selection

Considering algorithm 1 and algorithm 2 in section 3, σ , α and k play a crucial role in final result. These parameters can be various in different datasets. According to the Table1 in section 3.4, SURF feature is expected to have the best result. In our work, considering SURF method, we evaluated different σ , α values changing from 0.01 to 1 and calculated precision and recall respectively by retrieving related images in the dataset. As it can be seen in Table 3, the suitable parameter for σ , α values are 1 and 0.99, respectively. k shows the maximum number of edges for each vertex in k-RNN graph. It is logical that because there are 20 forged images in our dataset, the query vertex in k-RNN graph must have at least 20 edges and k has to be more than 20. By evaluating different k , we conclude that $k=35$ is the appropriate number.

Table 3: Parameters of manifold-ranking and k-RNN graph

Parameter	Value
α	0.99
σ	1
k	35

4.3. Evaluation Metrics

There are two important factors that have a great effect on image retrieval:1) quality and performance of the feature extraction algorithm. 2) the reliability of similarity computation. In this experiment, we evaluate the retrieval performance of CBIR based on the proposed approach by investigating three evaluation metrics: precision, recall and F-measure. A retrieval precision is defined as:

$$\text{Precision} = \frac{n_a}{n}$$

Where the total number of relevant images is denoted by n_a and n shows the total number of retrieved images. In this work we consider $n=15$.

The retrieval recall is defined as:

$$\text{Recall} = \frac{n_a}{n_b}$$

Where n_b denote the total number of relevant images in dataset. We set $n_b=20$ in our work. F-measure is computed based on both precision and recall of the test to calculate the score. It actually measures the image retrieval accuracy and which defined as follow:

$$F_measure = 2 \times \frac{\text{Precision} \times \text{Recall}}{\text{Precision} + \text{Recall}}$$

4.4. Manifold-Ranking based on k-RNN Graph Retrieval Performance Analysis

In the following experiments, four test images (Baboon, Lena, Pepper and Airplane) are used. Twelve main feature detectors and descriptors have been investigated and for each method, the average precision, recall and the F_measue are computed for the 20 images returned in retrieval result. As discussed above, the first measure, precision, is defined as the ratio of detected forged images among all forged images and the lower (near zero) value of this ration resulted in higher number of false charges of plagiarism and vice versa. Also, the ratio of detected actually forged images to all one reflects the recall measure. This exhibit the efficiency of detector and high value of this factor resulted in high sensibility of used method. The concept of F-measure is the weighted harmonic mean of its precision and recall. According to these interpretations, we considered two series in this work. First

series of tests is performed using six feature descriptors including SIFT, Root-SIFT, Jarret, SURF, GeoBlure and Scenc Gist. The similarity of test image based on selected feature detector with other images is computed by KLDiv metric. Then, after creating k-RNN graph and scoring each image by manifold-ranking, the retrieval result is validated by means of quality measurements, precision, recall and F_measure mentioned before. Fig.5, Fig.6 and Fig.7 demonstrate that the precision, recall and F_measure rates respectively. Considering all three metrics, Root-SIFT can indicate as the best detector by precision of 0.85, recall of 0.63 and F_measure of 1.9. In many cases such as large scale object retrieval, image classification, and repeatability under affine transformations, RootSIFT outperforms SIFT [47]. SIFT, SURF and Jarret also produced almost equally good result. The problem of other descriptors, especially Scene Gist and Geo Blur, is low either precision or recall factor which affect quality of performance.

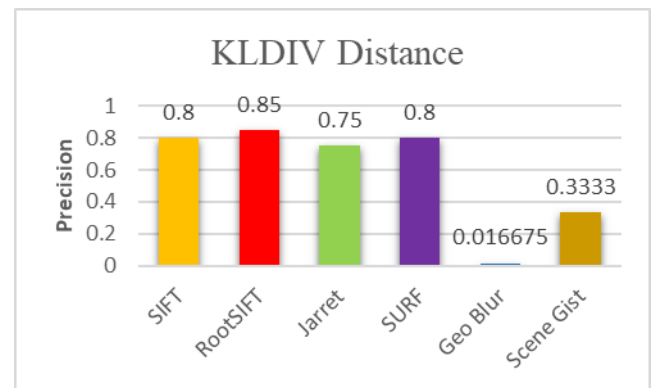


Fig. 5: Comparative result between methods measured by KLDIV

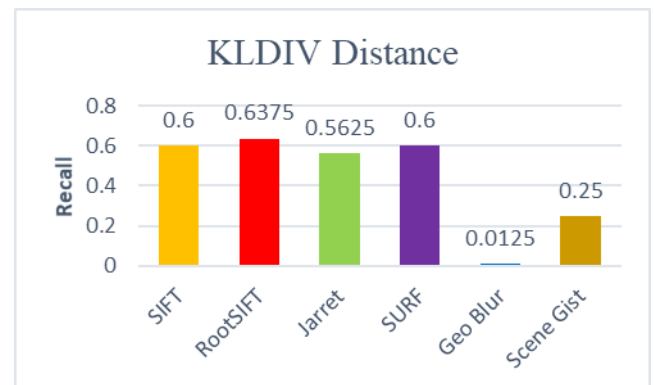


Fig. 6: Average Recall plot for methods measured by KLDIV

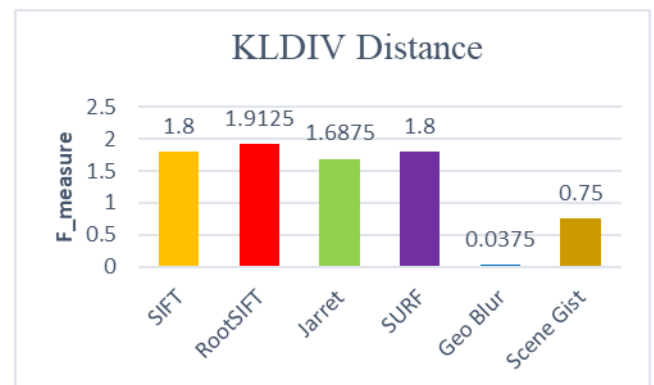


Fig. 7: Average F_measument plot for methods measured by KLDIV

The second six feature descriptors –HSV, EHD, ColorCorrelgram, Color Moment, LBP and Gabor- tested by precision, recall and F_measure metrics similar to the previous group discussed above. In this group Manhattan metric was considered to calcu-

late dissimilarity number. In this experiment, the average precision, recall and F-Measure were also computed and shown in Fig.10, Fig.11 and Fig.12 for second sixth methods. Gabor, EHD and LBP, due to apply filters in different directions (Horizontal, Vertical, Diagonal, Antidiagonal), have no robust performance in rotated forged images seen in Fig.8. We also analysis EHD, for instance, and present the results in Table 4. Considering six various scaled and rotated transformations, it can be concluded that EHD method due to applying filter in different directions has better result in scaling rather that rotation. It is true for other methods such as Gabor and LBP that uses filter in different directions. As it can be seen LBP has the lowest performance among all twelve methods. HSV, Color Moment and Color Correlgram perform very well; however, in the case that two pictures are similar in color but different in content such as Fig.9, these methods fail.

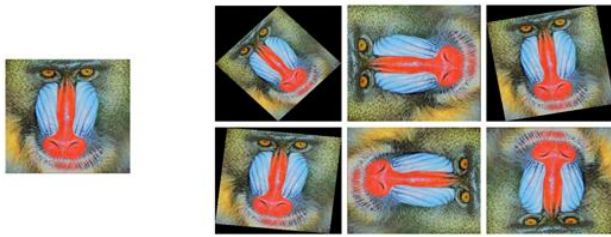


Fig. 8: Some rotated forged pictures that Gabor, EHD and LBP falls on them (a) Query image (b) Rotated images

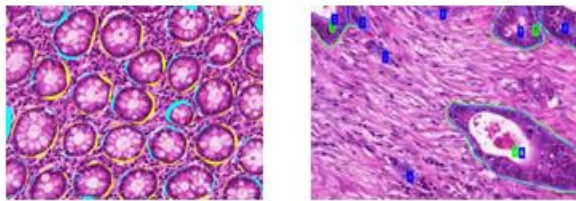


Fig. 9: Some same color pictures

Table 4: analysing EHD performance for different scale and rotation

Scale		Rotation	
Size	Manhattan Dis	Rotated Degree	Manhattan Dis
0.4 scaled	5.9843	270° L	7.7317
0.8 scaled	3.2479	180° L	9.3833
1.2 scaled	3.8401	45° L	8.9320
1.6 scaled	4.3367	10° L	5.6592
2 scaled	4.5075	10° R	4.6816
No scaled	0	90° R	9.0302
Ave of Scaling	3.65275	Ave of Rotation	7.5696

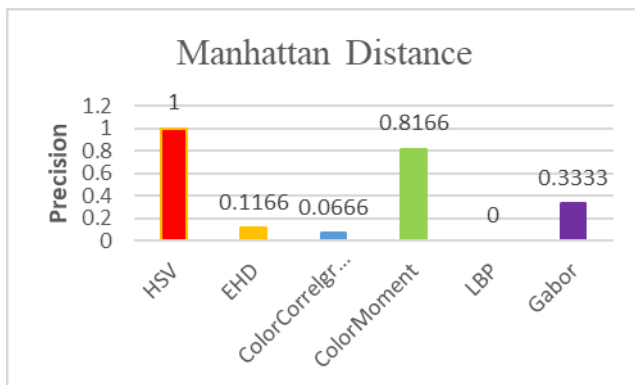


Fig. 10: Comparative result between methods measured by Manhattan

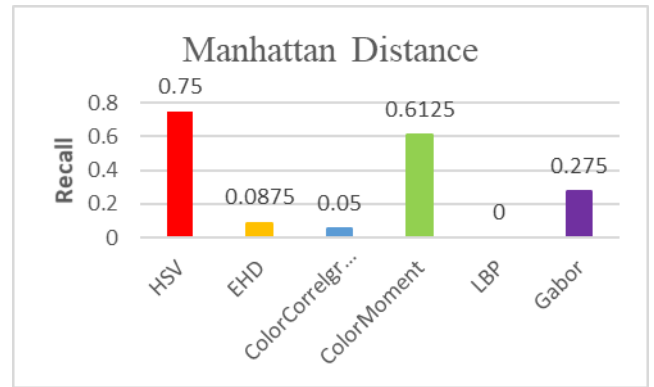


Fig. 11: Average Recall plot for methods measured by Manhattan

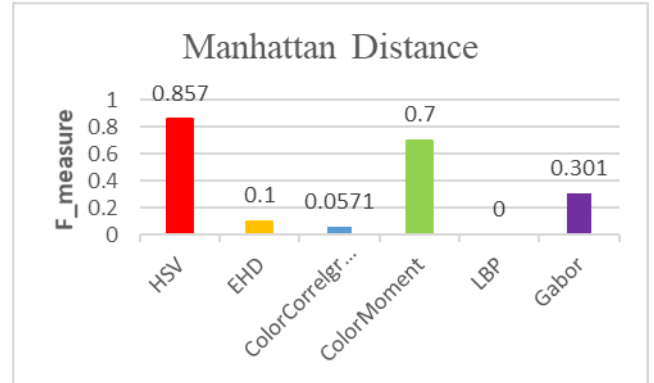


Fig. 12: Average F_measurement plot for methods measured by Manhattan

5. Conclusion

With ever-increasing development of image processing technology, detection of digital image forgery has become an area of focus in forensics science in recent years. In this paper, the functionality of manifold-ranking based on k-RNN graph by utilizing twelve various feature descriptors - SIFT, Root-SIFT, Jarret, SURF, GeoBlure, Scenc Gist, HSV, EHD, ColorCorrelgram, Color Moment, LBP and Gabor - are discussed, compared and analyzed. After extracting features, KIDiv and Manhattan metrics served to compute dissimilarity between images and the dissimilarity matrix is created as an input of k-RNN graph algorithm. Then each image is scored by k-RNN graph-based manifold-ranking. Given query image, the highest scored images are retrieved as forged images. Experimental results show that key point features offer better performance and among them RootSIFT effectively detects forgery invariant to rotation and scaling.

Appendix A. Dataset Setup

This appendix reflects a listing of parameters including rotation and resizing used to generate the manipulated images in our dataset.

- ❖ Rotation-only by θ
 - $\theta \in \{45^\circ, 90^\circ, 180^\circ, 270^\circ\}$
- ❖ Resizing-only (downscale or upscale) by scale factor s
 - Downscale $s \in \{20\%, 60\%\}$
 - Upscale $s \in \{20\%, 60\%, 100\%\}$
- ❖ Rotation by θ degrees + Resizing by scale factor s
 - Rotation θ + Downscale s

$$(\theta, s) \in \{(90^\circ, 60\%), (90^\circ, 20\%), (270^\circ, 10\%), (354^\circ, 50\%), (90^\circ, 30\%)\}$$

Rotation θ + Upscale s

$$(\theta, s) \in \{(80^\circ, 20\%), (90^\circ, 60\%), (270^\circ, 100\%), (270^\circ, 30\%), (10^\circ, 80\%), (270^\circ, 100\%)\}$$

References

- [1] D. Gupta "Study on Extrinsic Text Plagiarism Detection Techniques and Tools," *Journal of Engineering Science & Technology Review*, vol. 9, no. 5, 2016.
- [2] T. W. Chow and M. Rahman, "Multilayer SOM with tree-structured data for efficient document retrieval and plagiarism detection," *IEEE Transactions on Neural Networks*, vol. 20, no. 9, pp. 1385-1402, 2009.
- [3] Z. Su, B.-R. Ahn, K.-Y. Eom, M.-K. Kang, J.-P. Kim, and M.-K. Kim, "Plagiarism detection using the Levenshtein distance and Smith-Waterman algorithm," in *Innovative Computing Information and Control*, 2008. ICICIC'08. 3rd International Conference on, 2008, pp. 569-569: IEEE.
- [4] S. F. Hussain and A. Suryani, "On retrieving intelligently plagiarized documents using semantic similarity," *Engineering Applications of Artificial Intelligence*, vol. 45, pp. 246-258, 2015.
- [5] M. Elhadi and A. Al-Tobi, "Use of text syntactical structures in detection of document duplicates," in *Digital Information Management*, 2008. ICDIM 2008. Third International Conference on, 2008, pp. 520-525: IEEE.
- [6] B. Wang, F. Pan, K.-M. Hu, and J.-C. Paul, "Manifold-ranking based retrieval using k-regular nearest neighbor graph," *Pattern Recognition*, vol. 45, no. 4, pp. 1569-1577, 2012.
- [7] B. Xu, J. Bu, C. Chen, C. Wang, D. Cai, and X. He, "EMR: A scalable graph-based ranking model for content-based image retrieval," *IEEE Transactions on knowledge and data engineering*, vol. 27, no. 1, pp. 102-114, 2015.
- [8] Y. Fujiwara, G. Irie, S. Kuroyama, and M. Onizuka, "Scaling manifold ranking based image retrieval," *Proceedings of the VLDB Endowment*, vol. 8, no. 4, pp. 341-352, 2014.
- [9] Y. Wang, M. A. Cheema, X. Lin, and Q. Zhang, "Multi-manifold ranking: Using multiple features for better image retrieval," in *Pacific-Asia Conference on Knowledge Discovery and Data Mining*, 2013, pp. 449-460: Springer.
- [10] L. Ma, H. Li, F. Meng, Q. Wu, and L. Xu, "Manifold-ranking embedded order preserving hashing for image semantic retrieval," *Journal of Visual Communication and Image Representation*, vol. 44, pp. 29-39, 2017.
- [11] M. Iwanowski, A. Cacko, and G. Sarwas, "Comparing Images for Document Plagiarism Detection," in *International Conference on Computer Vision and Graphics*, 2016, pp. 532-543: Springer.
- [12] B. Neha, M. Mahajan, and S. Bhushan, "Comparison of Techniques for Plagiarism Detection in Document Images: A Review.," *European Journal of Advances in Engineering and Technology*, pp. 27-31, 2015.
- [13] D. G. Lowe, "Object recognition from local scale-invariant features," in *Computer vision*, 1999. The proceedings of the seventh IEEE international conference on, 1999, vol. 2, pp. 1150-1157: IEEE.
- [14] R. Arandjelović and A. Zisserman, "Three things everyone should know to improve object retrieval," in *Computer Vision and Pattern Recognition (CVPR)*, 2012 IEEE Conference on, 2012, pp. 2911-2918: IEEE.
- [15] H. Bay, T. Tuytelaars, and L. Van Gool, "Surf: Speeded up robust features," *Computer vision—ECCV 2006*, pp. 404-417, 2006.
- [16] A. C. Berg and J. Malik, "Geometric blur for template matching," in *Computer Vision and Pattern Recognition*, 2001. CVPR 2001. Proceedings of the 2001 IEEE Computer Society Conference on, 2001, vol. 1, pp. I-I: IEEE.
- [17] A. Oliva and A. Torralba, "Modeling the shape of the scene: A holistic representation of the spatial envelope," *International journal of computer vision*, vol. 42, no. 3, pp. 145-175, 2001.
- [18] M. A. Stricker and M. Orengo, "Similarity of color images," in *IS&T/SPIE's Symposium on Electronic Imaging: Science & Technology*, 1995, pp. 381-392: International Society for Optics and Photonics.
- [19] J. Huang, S. R. Kumar, M. Mitra, and W.-J. Zhu, "Image indexing using color correlograms," ed: Google Patents, 2001.
- [20] A. K. Jain and S. K. Bhattacharjee, "Address block location on envelopes using Gabor filters," *Pattern recognition*, vol. 25, no. 12, pp. 1459-1477, 1992.
- [21] A. K. Jain, N. K. Ratha, and S. Lakshmanan, "Object detection using Gabor filters," *Pattern recognition*, vol. 30, no. 2, pp. 295-309, 1997.
- [22] K. Jarrett, K. Kavukcuoglu, and Y. LeCun, "What is the best multi-stage architecture for object recognition?," in *Computer Vision*, 2009 IEEE 12th International Conference on, 2009, pp. 2146-2153: IEEE.
- [23] S. Park, D. Park, and C. Won, "Core experiments on MPEG-7 edge histogram descriptor," *MPEG document M*, vol. 5984, p. 2000, 2000.
- [24] D. K. Park, Y. S. Jeon, and C. S. Won, "Efficient use of local edge histogram descriptor," in *Proceedings of the 2000 ACM workshops on Multimedia*, 2000, pp. 51-54: ACM.
- [25] T. Ahonen, J. Matas, C. He, and M. Pietikäinen, "Rotation invariant image description with local binary pattern histogram fourier features," *Image analysis*, pp. 61-70, 2009.
- [26] B. Mahdian and S. Saic, "Detection of copy-move forgery using a method based on blur moment invariants," *Forensic science international*, vol. 171, no. 2, pp. 180-189, 2007.
- [27] Z. Mohamadian and A. A. Pouyan, "Detection of duplication forgery in digital images in uniform and non-uniform regions," in *Computer Modelling and Simulation (UKSim)*, 2013 UKSim 15th International Conference on, 2013, pp. 455-460: IEEE.
- [28] H. Farid, "Creating and detecting doctored and virtual images: Implications to the child pornography prevention act," *Department of Computer Science, Dartmouth College*, TR2004-518, vol. 13, 2004.
- [29] T. Zhang and R.-d. Wang, "Copy-move forgery detection based on SVD in digital image," in *Image and Signal Processing*, 2009. CISP'09. 2nd International Congress on, 2009, pp. 1-5: IEEE.
- [30] M. Zimba and S. Xingming, "DWT-PCA(EVD) Based Copy-move Image Forgery Detection," *International Journal of Digital Content Technology and its Applications*, vol. 5, no. 1, 2011.
- [31] S. Bravo-Solorio and A. K. Nandi, "Automated detection and localisation of duplicated regions affected by reflection, rotation and scaling in image forensics," *Signal Processing*, vol. 91, no. 8, pp. 1759-1770, 2011.
- [32] M. Sridevi, C. Mala, and S. Sandeep, "Copy-Move Image Plagiarism Detection," *Journal of Computer Science and Information Technology*, vol. 52, pp. 19-29, 2012.
- [33] H. Huang, W. Guo, and Y. Zhang, "Detection of copy-move forgery in digital images using SIFT algorithm," in *Computational Intelligence and Industrial Application*, 2008. PACIA'08. Pacific-Asia Workshop on, 2008, vol. 2, pp. 272-276: IEEE.
- [34] I. Amerini, L. Ballan, R. Caldelli, A. Del Bimbo, L. Del Tongo, and G. Serra, "Copy-move forgery detection and localization by means of robust clustering with J-Linkage," *Signal Processing: Image Communication*, vol. 28, no. 6, pp. 659-669, 2013.
- [35] R. C. Pandey, S. K. Singh, K. Shukla, and R. Agrawal, "Fast and robust passive copy-move forgery detection using SURF and SIFT image features," in *Industrial and Information Systems (ICIS)*, 2014 9th International Conference on, 2014, pp. 1-6: IEEE.
- [36] S. Prasad and B. Ramkumar, "Passive copy-move forgery detection using SIFT, HOG and SURF features," in *Recent Trends in Electronics, Information & Communication Technology (RTEICT)*, IEEE International Conference on, 2016, pp. 706-710: IEEE.
- [37] Y.-H. Lee and Y. Kim, "Efficient image retrieval using advanced SURF and DCD on mobile platform," *Multimedia Tools and Applications*, vol. 74, no. 7, pp. 2289-2299, 2015.
- [38] S. Jau-Ling and C. Ling-Hwei, "Color image retrieval based on primitives of color moments," *Recent Advances in Visual Information Systems*, pp. 19-27, 2002.
- [39] A. V. Malviya and S. A. Ladhake, "Pixel Based Image Forensic Technique for Copy-move Forgery Detection Using Auto Color Correlogram," *Procedia Computer Science*, vol. 79, pp. 383-390, 2016.
- [40] A. V. Malviya and S. A. Ladhake, "Region duplication detection using color histogram and moments in digital image," in *Inventive Computation Technologies (ICICT)*, International Conference on, 2016, vol. 1, pp. 1-4: IEEE.
- [41] C. H. Su, H. S. Chiu, J. H. Hung, and T. M. Hsieh, "Color Space Comparison between RGB and HSV Based Images Retrieval," in *Advanced Materials Research*, 2014, vol. 989, pp. 4123-4126: Trans Tech Publ.
- [42] R. P. Yohannan and M. Manuel, "Detection of copy-move forgery based on Gabor filter," in *Engineering and Technology (ICE-TECH)*, 2016 IEEE International Conference on, 2016, pp. 629-634: IEEE.

- [43] J.-C. Lee, "Copy-move image forgery detection based on Gabor magnitude," *Journal of Visual Communication and Image Representation*, vol. 31, pp. 320-334, 2015.
- [44] S. Agarwal, A. Verma, and P. Singh, "Content based image retrieval using discrete wavelet transform and edge histogram descriptor," in *Information Systems and Computer Networks (ISCON)*, 2013 International Conference on, 2013, pp. 19-23: IEEE.
- [45] L. Li, S. Li, H. Zhu, S.-C. Chu, J. F. Roddick, and J.-S. Pan, "An efficient scheme for detecting copy-move forged images by local binary patterns," *Journal of Information Hiding and Multimedia Signal Processing*, vol. 4, no. 1, pp. 46-56, 2013.
- [46] B. Ustubioglu, G. Ulutas, M. Ulutas, V. Nabiyev, and A. Ustubioglu, "LBP-DCT based copy move forgery detection algorithm," in *Information Sciences and Systems 2015*: Springer, 2016, pp. 127-136.
- [47] J. Winn, A. Criminisi, and T. Minka, "Object categorization by learned universal visual dictionary," in *Computer Vision, 2005. ICCV 2005. Tenth IEEE International Conference on, 2005*, vol. 2, pp. 1800-1807: IEEE.
- [48] T. Ojala, M. Pietikainen, and T. Maenpaa, "Multiresolution gray-scale and rotation invariant texture classification with local binary patterns," *IEEE Transactions on pattern analysis and machine intelligence*, vol. 24, no. 7, pp. 971-987, 2002.
- [49] A. Oliva, "Gist of the scene," *Neurobiology of attention*, vol. 696, no. 64, pp. 251-258, 2005.
- [50] Y. Rubner, C. Tomasi, and L. J. Guibas, "The earth mover's distance as a metric for image retrieval," *International journal of computer vision*, vol. 40, no. 2, pp. 99-121, 2000.
- [51] C.-T. Hsieh, J.-L. Shih, C.-H. Lee, C.-C. Han, and K.-C. Fan, "3D model retrieval using multiple features and manifold ranking," in *Ubi-Media Computing (UMEDIA)*, 2015 8th International Conference on, 2015, pp. 7-10: IEEE.
- [52] C. Zhang and F. Wang, "A multilevel approach for learning from labeled and unlabeled data on graphs," *Pattern Recognition*, vol. 43, no. 6, pp. 2301-2314, 2010.
- [53] J. He, M. Li, H.-J. Zhang, H. Tong, and C. Zhang, "Manifold-ranking based image retrieval," in *Proceedings of the 12th annual ACM international conference on Multimedia*, 2004, pp. 9-16: ACM.